The Ultrafast Charge-Transfer-to-Solvent Dynamics of Iodide in Tetrahydrofuran. 1. Exploring the Roles of Solvent and Solute Electronic Structure in Condensed-Phase Charge-Transfer Reactions[†]

Arthur E. Bragg and Benjamin J. Schwartz*

Department of Chemistry and Biochemistry, University of California, Los Angeles, Los Angeles, California 90095-1569

Although they represent the simplest possible charge-transfer reactions, the charge-transfer-to-solvent (CTTS) dynamics of atomic anions exhibit considerable complexity. For example, the CTTS dynamics of iodide in water are very different from those of sodide (Na$^-$) in tetrahydrofuran (THF), leading to the question of the relative importance of the solvent and solute electronic structures in controlling charge-transfer dynamics. In this work, we address this issue by investigating the CTTS spectroscopy and dynamics of I$^-$ in THF, allowing us to make detailed comparisons to the previously studied I$^-$/H$_2$O and Na$^-$/THF CTTS systems. Since THF is weakly polar, ion pairing with the counterion can have a substantial impact on the CTTS spectroscopy and dynamics of I$^-$ in this solvent. In this study, we have isolated "counterion-free" I$^-$ in THF by complexing the Na$^+$ counterion with 18-crown-6 ether. Ultrafast pump−probe experiments reveal that THF-solvated electrons (e^-_{THF}) appear 380 ± 60 fs following the CTTS excitation of "free" I$^-$ in THF. The absorption kinetics are identical at all probe wavelengths, indicating that the ejected electrons appear with no significant dynamic solvation but rather with their equilibrium absorption spectrum. After their initial appearance, ejected electrons do not exhibit any additional dynamics on time scales up to ∼1 ns, indicating that geminate recombination of e^-_{THF} with its iodine atom partner does not occur. Competitive electron scavenging measurements demonstrate that the CTTS excited state of I$^-$ in THF is quite large and has contact with scavengers that are several nanometers away from the iodide ion. The ejection time and lack of electron solvation observed for I$^-$ in THF are similar to what is observed following CTTS excitation of Na$^-$ in THF. However, the relatively slow ejection time, the complete lack of dynamic solvation, and the large ejection distance/lack of recombination dynamics are in marked contrast to the CTTS dynamics observed for I$^-$ in water, in which fast electron ejection, substantial solvation, and appreciable recombination have been observed. These differences in dynamical behavior can be understood in terms of the presence of preexisting, electropositive cavities in liquid THF that are a natural part of its liquid structure; these cavities provide a mechanism for excited electrons to relocate to places in the liquid that can be nanometers away, explaining the large ejection distance and lack of recombination following the CTTS excitation of I$^-$ in THF. We argue that the lack of dynamic solvation observed following CTTS excitation of both I$^-$ and Na$^-$ in THF is a direct consequence of the fact that little additional relaxation is required once an excited electron nonadiabatically relaxes into one of the preexisting cavities. In contrast, liquid water contains no such cavities, and CTTS excitation of I$^-$ in water leads to local electron ejection that involves substantial solvent reorganization.

I. Introduction

The charge-transfer-to-solvent (CTTS) dynamics of simple anions have received a great deal of recent interest as a means to interrogate how the structure and dynamics of local solution environments dictate the outcome of chemical reactions in liquids[1−28] and clusters.[29−36] The valence electrons of CTTS anions are bound by the nucleus in the ground state, but the excited states are bound only by the polarization of the surrounding solvent. Thus, the CTTS label is somewhat of a misnomer; excitation of a CTTS transition (see, e.g., Figure 1a and c, below) does not directly transfer the excess electron to the solvent. Instead, solvent motions subsequent to creation of

the solvent-supported excited state lead to charge transfer, generating solvated electrons, e^-_{solv}

$$\mathrm{A}^- \xrightarrow{h\nu} \mathrm{A}^{-*} \xrightarrow{\mathrm{CTTS}} \mathrm{A} + e^-_{\mathrm{solv}}$$
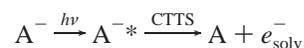
where A$^-$ represents a CTTS anion. Consequently, both the steady-state spectroscopy and the dynamics of the CTTS electron ejection process provide sensitive probes of the local solution environment.

Most of the attention given to CTTS systems has focused on atomic anions as they lack internal (nuclear) degrees of freedom. Thus, any spectroscopic dynamics associated with CTTS electron ejection from atomic ions must directly reflect the motions of solvent molecules. To this end, the CTTS behavior of solvated I$^-$, including its steady-state spectroscopy in various solution environments,[37−46] photoinduced electron yields,[3,47−52]
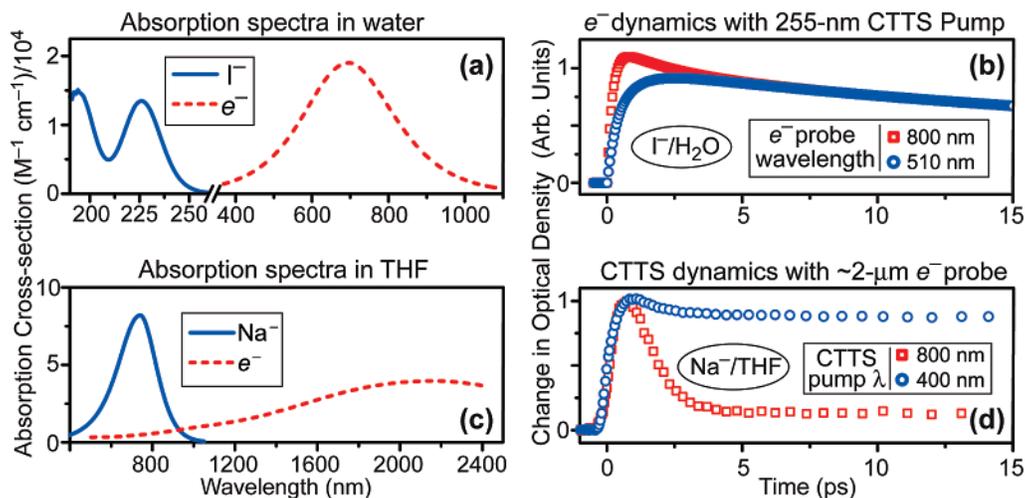
Figure 1. The spectroscopy and dynamics of the I⁻/H₂O and Na⁻/THF CTTS systems. (a) Absorption spectra of aqueous I⁻ (blue solid curve) and the hydrated electron (red dashed curve, ref 55). (b) Ultrafast $e^-_{H_2O}$ absorption transients associated with the 255 nm CTTS excitation of aqueous I⁻; the data points were generated from analytic fits presented in ref 2. The transient dynamics are probe-wavelength-dependent (cf. 510 nm probe (blue circles) and 800 nm probe (red squares)) but are pump-wavelength-independent across the lowest-energy CTTS band of I⁻ (not shown; see ref 5). (c) Absorption spectra of Na⁻ in THF (blue solid curve, ref 56) and e^-_{THF} (red dashed curve, ref 57). (d) Ultrafast e^-_{THF} absorption transients measured following both 400 (blue circles) and 800 nm (red squares) CTTS excitation of Na⁻ in THF (ref 14). Although the e^-_{THF} transients are pump-wavelength-dependent, they are probe-wavelength-independent (not shown).

and ultrafast electron-transfer dynamics,[1−5,8,9,28] has been characterized extensively over the last 75 years. Figure 1a shows the CTTS absorption spectrum of aqueous I⁻ (blue solid curve), which consists of two broad and featureless bands that peak at 225 and 193 nm; these bands are associated with the two spin−orbit states ($^2P_{3/2}$ and $^2P_{1/2}$) of the neutral I atom photoproduct.[41] The dynamics following one-photon CTTS excitation of I⁻ in polar liquids has been investigated extensively by Bradforth and co-workers[1−5,7,8] (as well as by others[9,28]). A small subset of Bradforth and co-workers' ultrafast spectral measurements associated with the CTTS excitation of aqueous I⁻ are highlighted in Figure 1b;[53] excitation of the I⁻ CTTS band leads to the rapid (<100 fs) appearance of hydrated electrons with a near-unit quantum yield.[3] The newly ejected electrons are formed out of equilibrium and thermalize on a ~1 ps time scale;[4] the decay at red wavelengths (Figure 1b, red squares) and the corresponding rise at blue wavelengths (Figure 1b, blue circles) indicate a dynamic spectral blue-shift that reflects the equilibration of the ejected hydrated electron (the equilibrated $e^-_{H_2O}$ spectrum is plotted as the red dashed curve in Figure 1a[54,55]). A significant fraction of the ejected electrons, which reside in I/e^-_{solv} contact pairs, subsequently recombine with their I atom parents on an approximately tens-of-picoseconds time scale.[2] All of the dynamics are independent of the wavelength used to excite the lowest-energy CTTS band.[5]

In addition to these investigations of the I⁻ CTTS behavior in polar, protic solvents, the ultrafast CTTS dynamics of sodium anions, or sodide (Na⁻), in weakly polar, aprotic solvents has been studied in experiments both by Schwartz and co-workers[10−16,22] and by Ruhman and co-workers.[20,21] In liquid tetrahydrofuran (THF), Na⁻ has a CTTS band that peaks near 720 nm (blue solid curve, Figure 1c),[56] a spectral region that is conveniently accessed with modern Ti:Sapphire lasers. Figure 1d demonstrates that excitation of the Na⁻ CTTS band produces e^-_{solv} (whose equilibrium spectrum in THF is shown as the red dashed curve in Figure 1c[57]), but with an appearance time of ~450 fs.[19,22] Perhaps more striking is the fact that the spectral dynamics are identical at all probe wavelengths (not shown), indicating that the ejected THF-solvated electrons appear at

equilibrium.[12,19,22] The equilibrated solvated electrons then recombine with their geminate Na⁰ partners on two time scales, a fast back electron transfer that is complete within ~1 ps and a slower transfer that takes place on a ~200 ps time scale. These processes have been assigned as arising from the recombination of immediate and solvent-separated Na⁰/e^-_{solv} contact pairs, respectively.[12,18] Figure 1d also demonstrates that the recombination dynamics following the CTTS excitation of Na⁻ are highly sensitive to excitation wavelength, with fewer electrons recombining on either time scale as the excitation energy is increased,[13] even though the electron ejection dynamics are independent of excitation wavelength.[19,22]

The data highlighted in Figure 1 pose an obvious question: Why are the CTTS ejection and recombination dynamics of aqueous I⁻ so different from those of Na⁻ in THF? Do the differences in electron ejection time, post-ejection electron thermalization dynamics, recombination kinetics, and excitation wavelength dependence result primarily from differences in the solvent or the solute, or possibly from a combination of both? The logical way to address this question would be to cross the roles of the solute and solvent by studying either aqueous Na⁻ or I⁻ in THF. Of course, sodium metal reacts violently with water, such that aqueous Na⁻ is experimentally inaccessible (although we have studied the aqueous Na⁻ CTTS system via computer simulation[23]). Thus, in this paper, we address the intersecting roles of the solute and solvent in the CTTS process by examining the ultrafast dynamics associated with the CTTS excitation of I⁻ in liquid THF.

In some respects, the fact that the CTTS dynamics of I⁻ and Na⁻ are so different is not all that surprising. The ground state of I⁻ has its valence electron in a 5p orbital, such that one-photon CTTS excitation reaches a single s-like state supported by the surrounding solvent cavity.[58] The electronic structure of Na⁻, however, is inverted relative to that of I⁻; the Na⁻ CTTS band has been assigned to the promotion of an electron from a 3s ground state to one of three orthogonal, solvent-bound p-like excited states, the degeneracy of which is broken by the asymmetry of the local solvent environment.[12,20,21,23] This symmetry difference has important implications for the electron

Ultrafast CTTS Dynamics of Iodide in THF

J. Phys. Chem. B, Vol. 112, No. 2, 2008 **485**

detachment process; since the ground state of a solvated electron is s-like, detachment from the s-like CTTS excited state of I^- can occur directly, but detachment following the CTTS excitation of Na^- requires a nonadiabatic transition to remove the node from the Na^- p-like CTTS excited state(s).[23] The differing electronic symmetries of I^- and Na^- also likely play a role in recombination, as a nonadiabatic transition is required to regenerate the I^- 5p ground state from the s-like ground state of e^-_{solv},[24] but no such transition is required for recombination to produce the Na^- 3s ground state.[23]

Of course, we also expect that the dynamics observed following CTTS excitation should depend as much on local solvent structure and dynamics as on the electronic structure of the CTTS anion. For example, molecular dynamics simulations from our group predicted[59] and neutron diffraction experiments recently confirmed[60] that liquid THF naturally contains relatively large solvent voids that are close in size to that of the solvated electron. These voids, or cavities, result from inefficient packing of THF molecules in the liquid. Moreover, the way in which the THF molecules pack produces a net positive electrostatic potential within these solvent cavities, such that liquid THF is naturally filled with preexisting electron traps.[59] Additionally, our simulations suggest that the excited-state wave functions of THF-solvated electrons have considerable amplitude in the preexisting cavities that are spatially proximal to the cavity occupied by the ground-state e^-_{THF} wave function.[59] We refer to such multicavity excited states as having "disjoint" character, and both simulations[61] and experiments[15,16,19] have shown that excitation of a THF-solvated electron leads to relocalization, where the electron relaxes into a new cavity that can be quite far (possibly up to several nanometers) from its original location. These observations suggest that the reason that little solvent relaxation is observed following CTTS excitation of Na^- in THF is because electron ejection takes place into one of these preexisting electron traps in liquid THF; the electron ejection kinetics are rate-limited by the time it takes the electron to relax into a preexisting cavity from one of the disjoint solvent-supported excited states, not by the time for solvation to occur once the cavity is occupied.[22] In contrast, the tightly packed structure of liquid water does not contain preexisting voids,[62] such that any relocalization[63,64] or other accommodation of a new aqueous electron requires substantial solvent reorganization, as observed both in the aqueous I^- CTTS process[1,2,4,24,25] and in the relaxation of excited hydrated electrons.[2,4,65−69]

The presence of preexisting electron traps in liquid THF also can explain the change in Na^- CTTS recombination dynamics with excitation energy; excitation at higher energies increases the probability that the initially created CTTS excited state can couple with a disjoint electronic state encompassing other cavities, thus increasing the probability that the excited electrons localize further from the Na^0 core.[22] On the other hand, it is unclear how the s-like CTTS excited state of I^-, which in water has been described as an asymmetrically shaped orbital that is larger and more nonspherical than an equilibrated hydrated electron,[58] would be affected by coupling to the low-lying disjoint states that exist as a natural part of the electronic structure of liquid THF. How sensitive is the CTTS excited-state wave function of I^- in THF to the instantaneous distribution of solvent voids in proximity to the parent solute? Will the relaxation of the I^- CTTS excited state in THF involve a nonadiabatic cascade through disjoint solvent-supported electronic states, or is another mechanism involved that might be more similar to that observed in water? How is recombination of the ejected electron with its iodine atom parent, which in

water has been described as a competition between diffusive escape on a potential of mean force and back electron transfer,[3,5] altered in THF?

In this paper, we address all of these issues by investigating the ultrafast CTTS dynamics of I^- in THF. One key issue involved in studying the I^- CTTS process in THF is the role of the iodide salt counterion. In water, the I^- CTTS spectrum and dynamics are not affected by the presence (and identity) of the counterion up to millimolar concentrations,[2,9] and there are no qualitative differences in I^- CTTS dynamics observed at high ionic strength.[7] In contrast, the CTTS spectrum of I^- in THF shifts significantly when the cation is changed,[40] portending that considerable differences in CTTS dynamics also may exist. We will explore in detail how the CTTS ejection and recombination dynamics are altered with the identity of the counterion associated with the dissolved I^- solute in THF in a future paper.[70] In this contribution, we examine the CTTS dynamics of I^- in THF under "counterion-free" conditions; by complexing the Na^+ counterion with a cyclic crown ether, we ensure that ion pair interactions between the countercation and the I^- anion are screened and negligibly affect the I^- CTTS dynamics.

The rest of this paper is organized as follows. Section II outlines our experimental methods, including considerable detail regarding sample preparation and purity. In section III.A, we discuss the counterion dependence of the I^- CTTS band and demonstrate how the use of cation complexing agents allows us to create "counterion-free" I^- in this solvent. In section III.B, we show that the CTTS ejection of electrons from I^- in THF takes ∼400 fs and that the electrons appear with their equilibrated spectrum, just as is the case for Na^-. Unlike the case of both Na^- in THF and I^- in water, however, we show that negligible geminate recombination takes place on subnanosecond time scales. In section III.C, we describe scavenging experiments that allow us to estimate the spatial extent of the ejected electron distribution following the CTTS excitation of I^- in THF, and in section III.D, we show that CTTS electrons are ejected farther from their parents than are electrons ejected upon multiphoton ionization of the neat solvent. We close in section IV by presenting a scheme that allows us to understand not only these observations but all of the differences between the I^-/H_2O, Na^-/THF, and I^-/THF CTTS systems and how these differences depend on the electronic structure of both the solute and solvent.

II. Experimental Section

One significant issue for all of the experiments reported below is that of sample purity, particularly involving the tetrahydrofuran (THF) solvent used in all of the solutions. THF, like most peroxide-forming ethers, is typically sold containing a small amount of a free-radical inhibitor, such as butylated hydroxytoluene (BHT). The presence of BHT is problematic for ultrafast CTTS measurements for two reasons; first, BHT acts as an electron scavenger, potentially altering the observed dynamics of the solvated electrons ejected via the CTTS process. Second, as shown in Figure 2, BHT in THF (as purchased from Fischer) has an optical absorption (black solid curve) with bands at ∼220 and ∼280 nm that overlap the I^- CTTS band (black circles). Thus, all of the THF used in our experiments was purified by drying over potassium metal under an Ar atmosphere and distilling freshly before use. The absorption spectrum of freshly distilled THF is shown as the blue dashed curve in Figure 2 and is optically transparent down to ∼210 nm. All of the absorption spectra presented in this paper were measured with a Perkin-Elmer Lambda 25 UV−vis spectrometer using 1 mm
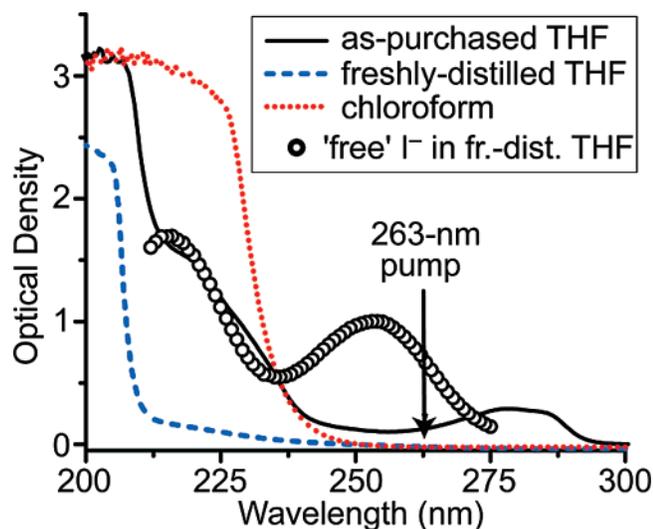
Figure 2. Absorption spectra of the solutes and solvents used in this study: absorption spectrum of BHT-stabilized THF (black solid curve); absorption spectrum of freshly distilled THF (blue dashed curve); absorption spectrum of chloroform (red dotted curve); absorption spectrum of "counterion-free" I^- in THF (black circles; see the text in section III.A for details on obtaining the "counterion-free" I^- CTTS spectrum).

path length quartz cuvettes; I^- spectra were measured relative to a "blank" of freshly distilled THF.

In addition to solvent stabilizers, the presence of oxygen in the samples is also problematic. Not only is oxygen an efficient electron scavenger, but the addition of iodide salts to oxygenated THF leads to oxidation of I^- to produce a significant amount of I_3^-, particularly upon exposure to UV light. Triiodide also acts as an electron scavenger at high concentrations and absorbs strongly in the near-UV at both ~290 and ~360 nm.[71] Fortunately, the steady-state spectroscopy and ultrafast spectroscopic signatures associated with the excitation of I_3^- in solution are well understood,[71-73] such that contaminated samples readily could be identified. To avoid problems with the buildup of I_3^- in the samples, we circulated our sample solutions through a closed-loop system consisting of a 2 mm path length quartz flow cell (Spectrocell) and Teflon tubing using a peristaltic pump (Cole-Parmer), thus diluting any pump-induced byproducts into a large solution volume and providing a fresh sample for every laser shot. If we flushed the entire flow system with N_2 gas prior to introduction of the sample, we found that buildup of I_3^- was negligible over the course of several hours, as verified both spectroscopically and by the similarity of pump-probe data taken before and after several hours of exposure of the samples to UV laser pulses. We prepared fresh solutions daily and whenever we judged that the level of accumulated byproduct or contaminants became unacceptable. The preparation of our solutions was done in a nitrogen glove box and involved dissolving NaI (Fluka, >99.5% purity, used as received) and 18-crown-6 cyclic ether (1,4,7,10,13,16-hexaoxacyclooctadecane, 18C6, Aldrich, >98% purity, used as received) in freshly distilled THF to prepare 150-200 mL of a ~10 mM NaI solution; the solutions were mixed via moderate sonication and modest heating in sealed flasks.

In addition to the I^-/THF solutions, we also prepared solutions to perform a series of electron scavenging experiments (described in more detail in section III.C) by adding controlled quantities of chloroform ($CHCl_3$). For these experiments, we used spectroscopic-grade chloroform (OmniSolv), which was

deoxygenated by repeated freeze-pump-thaw cycles. The red dotted curve in Figure 2 demonstrates that the optical absorption of chloroform does not overlap with the lowest-energy I^- CTTS transition (black circles). Solutions were prepared by serially adding known volumes of air-free chloroform to a NaI/18C6/THF solution of known volume (150 mL) and concentration. These solutions were subsequently stirred for 35-45 min within the closed flow circuit before irradiating with laser pulses. In the presence of $CHCl_3$, we found that reaction byproducts slowly built up on the flow cell wall at the point of laser irradiation, attenuating the pump pulse as it entered the sample. As a remedy, we manually rastered the flow cell through the laser interaction region in directions perpendicular to the pump laser beam prior to each individual pump-probe scan. With this technique, we obtained identical absorption transients over multiple measurements at each chloroform concentration. We determined relative static quenching yields by coupling time-resolved measurements with a series of measurements in which the laser overlap and sample position relative to beam focus were unaltered while we measured the concentration-dependent absorption intensity at a fixed temporal delay ($t = 20$ ps). This allowed us to accurately scale the time-resolved scavenging transients at this delay according to the measured fixed-delay absorption intensities.

The details of our femtosecond pump-probe transient absorption setup have been published previously.[74] Pump and probe pulses were derived from a regeneratively amplified Ti: sapphire laser (Spectra Physics) outputting ~120 fs pulses centered near 790 nm with an ~800 μJ pulse energy at a 1 kHz repetition rate. One-third of this beam (~250 μJ) was used to generate 263 nm pump pulses (~3-5 μJ) by first doubling the 790 nm output in a BBO crystal and then mixing the resultant 395 nm light with the remaining 790 nm beam in a second crystal. Two-thirds of the amplifier output was used to pump a dual-pass optical parametric amplifier (OPA, Spectra Physics), creating tunable signal and idler beams in the 1.2-2.5 μm region that were isolated and used directly as IR probes. Visible probe pulses were generated by doubling the signal output. The relative pump-probe polarization for visible probe colors was controlled using a half-wave plate/polarizer pair and set to the magic angle (54.7° relative polarization). We could not set the relative UV-IR polarization to the magic angle, but we found that IR transients recorded at both 0 and 90° relative polarization exhibited the same time dependence at all of our chosen probe wavelengths. The probe beam was directed onto a computer-controlled, variable-delay translation stage (Newport) outfitted with a corner-cube reflector. The pump and probe beams were collinearly recombined off of a 266 nm high reflector and were focused toward the sample with a 100 mm fused-silica lens, with the flow cell placed 2-5 cm before the pump focus. The probe beam was collimated prior to recombination with a 1 m lens to ensure that the probe spot size (~50-100 μm diameter) was well within the pump spot size (~200 μm diameter). Visible absorption transients were measured with Si photodiodes (Thorlabs DET-100), and IR transients were recorded using either InGaAs photodiodes (Thorlabs DET-400) or InAs photodetectors (Judson Technologies), as appropriate for the wavelength. A mechanical chopper was placed in the pump path to actuate pump-on/pump-off detection. A small portion of the probe beam was split off prior to the sample and was directed to a reference detector for shot-by-shot double normalization, whereby the intensity of the probe pulse transmitted through the sample was divided by the intensity measured on the reference detector both with and without the pump pulse

Ultrafast CTTS Dynamics of Iodide in THF

J. Phys. Chem. B, Vol. 112, No. 2, 2008 **487**
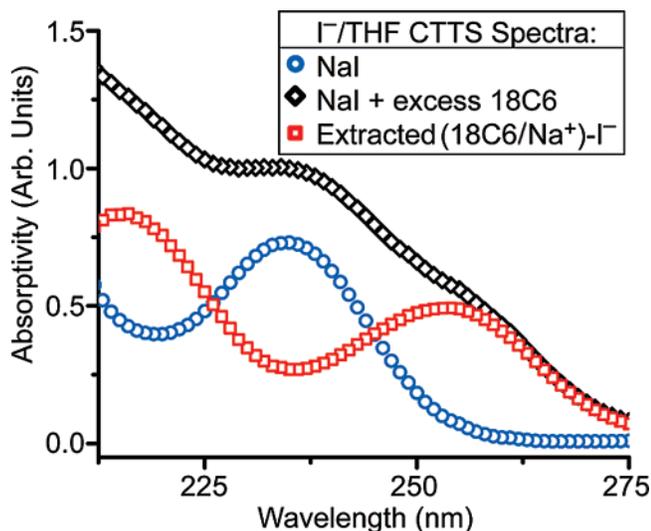
Figure 3. The steady-state CTTS spectroscopy of I$^-$ in THF in the region red of 210 nm (below which the solvent strongly absorbs): absorption spectrum of NaI in THF (blue circles); absorption spectrum of NaI in THF in the presence of excess 18-crown-6 ether (black diamonds); absorption spectrum of (18C6/Na$^+$)−I$^-$ ("counterion-free" I$^-$, red squares). The "counterion-free" spectrum was obtained through conditioned subtraction of the NaI and 18C6 + NaI spectra, as described in the text; the spectra are plotted to reflect the relative contribution of NaI (blue circles) and (18C6/Na$^+$)−I$^-$ (red squares) to the measured composite spectrum (black diamonds).

present.[74] This detection scheme normalizes for fluctuations in the probe beam intensity and permits measurement of signals as small as $\Delta OD \sim 10^{-4}$ with a few hours of signal averaging. Signals presented here were collected over 30 min to 2 h. Associated error bars were determined from the 95% confidence limits of the mean. All of the experiments were performed at room temperature.

As we will discuss in more detail in a subsequent paper,[70] the relatively long path length of our flow cell, combined with the index of refraction mismatch in THF between the UV-pump and IR-probe wavelengths used in our experiments, has the potential to alter the measured transient signals at early times, introducing a "lazy" signal rise due to group velocity mismatch (GVM) through the sample. For the experiments presented here, the absorptivity at 263 nm was high enough to ensure negligible penetration of the pump beam into the flow cell, such that GVM negligibly affected the measured signal rise. We found no dependence of any of the measured spectroscopic signals on the I$^-$ concentration of the sample (1−20 mM) or on the intensity of the pump pulse (10^{-3}−10^{-2} J/cm^2).

III. Results: The Steady-State Spectroscopy and Ultrafast CTTS Dynamics of I$^-$ in THF

A. Extracting the Steady-State CTTS Absorption Spectrum of "Counterion-Free" I$^-$ in THF. One of the hallmarks of CTTS transitions is their extraordinary sensitivity to the local environment of the CTTS anion; CTTS band positions are affected by solvent identity, the ionic strength of the solution, and the addition of cosolutes and cosolvents.[41] This sensitivity results directly from the fact that the CTTS excited state is entirely solvent-supported, such that small changes in the size, shape, and/or polarity of the solvent cavity surrounding the CTTS solute can have large effects on the CTTS transition energy. Since solvent-supported CTTS excited states are similar in character to the solvent-supported excited states of solvated

electrons, it is perhaps not surprising that there exists a strong correlation between CTTS transition energies and those of solvated electrons in the same environments. For example, Fox and Hayon correlated the absorption maxima of the (lower-energy) I$^-$ CTTS transition and the solvated electron's spectrum in 30 solvent systems and found a linear relationship of the form[75]

$$\nu_{max}(e_{solv}^-) = [\nu_{max}(I_{solv}^-) \cdot 1.65 - 60.0] \times 10^3 \text{ cm}^{-1} \quad (2)$$

Thus, given the THF-solvated electron's absorption maximum of 2160 nm (4630 cm^{-1}) (cf. Figure 1c), eq 2 predicts a CTTS absorption maximum of 39200 cm^{-1} (255 nm) for I$^-$ in THF.[76]

The blue circles plotted in Figure 3 give the steady-state absorption spectrum of NaI in THF. The spectrum exhibits the characteristic band shape of an I$^-$ CTTS transition, with the maximum of the lowest-energy absorption feature at 235 nm. This peak position is red-shifted ~1935 cm^{-1} relative to that in water ($\epsilon = 78$, cf. Figure 1a) due to the lower polarity of THF ($\epsilon = 7.5$). The 235 nm absorption maximum, however, is still blue-shifted ~20 nm (~3300 cm^{-1}) relative to what we expect from the empirical correlation of eq 2. Thus, the position of the NaI CTTS band maximum in THF strongly suggests that the Na$^+$ counterion significantly perturbs the local environment relative to that of "free" I$^-$.[40] In fact, conductivity measurements reveal that Na$^+$ salts are largely ion paired in THF at millimolar concentrations ($K_{diss} \sim 10^{-6}$ M);[77,78] therefore, we expect a significant degree of ion pairing between Na$^+$ and I$^-$.[79] Thus, the blue shift of the CTTS band of NaI relative to that expected for "free" I$^-$ makes sense since the presence of the nearby Na$^+$ should create a more polar environment around the anion.[40] Having the cation nearby the anion also leads to dramatic changes in I$^-$ CTTS dynamics, as we will discuss in detail in a future publication.[70]

As our focus here is to investigate the CTTS behavior of "counterion-free" I$^-$, it is necessary to screen the coulomb interaction in the Na$^+$−I$^-$ ion pair, preferably with a method that drives the ion-pairing equilibrium toward dissociation. To this end, we added excess 15-crown-5 (1,2,7,10,13-pentaoxa-cyclopentadecane, 15C5) and 18-crown-6 (18C6) cyclic ethers to our NaI/THF solutions, both of which are known to be good chelating agents for Na$^+$. We found that the addition of 15C5 induced significant precipitation, leaving a dilute solution that had the same CTTS spectrum as that of the NaI/THF solution with no added 15C5. This behavior likely results from a very high binding affinity of 15C5 for Na$^+$ and a relatively low solubility of the (15C5/Na$^+$)−I$^-$ complex in THF. On the other hand, we found that the addition of 18C6 had no negative effects on the solubility of NaI in THF and, more importantly, that the addition of 18C6 led to significant changes in the NaI/THF CTTS absorption spectrum. The black diamonds in Figure 3 show that chelating the Na$^+$ with 18C6 leads to the growth of shoulders on both the red and blue sides of the lowest-energy Na$^+$−I$^-$ CTTS absorption peak. Thus, the addition of 18C6 leads to what appears to be a superposition of the NaI/THF spectrum and something new, presumably the spectrum of I$^-$ corresponding to 18C6-complexed Na$^+$.

To obtain the spectrum of this new feature, we subtracted the spectrum of Na$^+$−I$^-$ in THF from that of the NaI/18C6/THF solution. Unfortunately, there is no obvious way to scale the Na$^+$−I$^-$ spectrum for subtraction, as it lies well within the measured composite spectrum. Therefore, as a condition for subtraction, we stipulated that the intensity ratio of the first absorption maximum of the extracted (18C6/Na$^+$)−I$^-$ band to

the first minimum above this band must match the same ratio (0.55) measured from the Na^+-I^- spectrum. The $(18C6/Na^+)-I^-$ spectrum that we obtained from this conditioned decomposition is plotted with red squares in Figure 3.[80] The resultant spectrum demonstrates that complexing Na^+ significantly red shifts (by $\sim$3230 cm^{-1}) the lowest-energy peak of the I^- CTTS spectrum to 254 nm, nearly the position predicted for the CTTS spectrum of "free" I^- from eq 2, indicating that the addition of 18C6 allows us to produce "counterion-free" I^- in THF.[81] Even though we are unable to complex all of the Na^+ counterions, the spectrum of the "counterion-free" I^- is red-shifted sufficiently from that of Na^+-I^- that it is straightforward to spectrally select "counterion-free" I^- in our time-resolved experiments by exciting solutions at 263 nm, a wavelength at which the Na^+-I^- ion pair absorbs only weakly (cf. Figure 3).

B. The Ultrafast CTTS Dynamics of "Counterion-Free" I^- in THF. Now that we have demonstrated the ability to make and spectrally select "counterion-free" I^- in weakly polar solvents, we turn next to pump−probe experiments aimed at examining the dynamic spectroscopy that follows the CTTS excitation of I^- in THF. Time-resolved absorption transients measured after the 263 nm CTTS excitation of "free" I^- in THF and probed at selected wavelengths in the near-infrared and visible, where the THF-solvated electron absorbs,[82] are plotted in Figure 4. Figure 4a indicates that all of the measured spectral transients are identical within the measured error bars at the earliest delays. This observation is strikingly different than what was observed for the dynamics of aqueous I^- (cf. Figure 1b). However, as inferred previously for the CTTS ejection of electrons from Na^- in THF,[19,22] the data in Figure 4a indicate that nascent electrons ejected after the CTTS excitation of I^- appear with their equilibrium absorption spectrum. This observation is consistent with the idea that liquid THF is full of preexisting cavities that act as electron traps[59,60] and that the little structural reorganization of the solvent required to accommodate the ejected electron occurs more rapidly than the time scale for electron ejection.

To determine the time it takes for electrons to relax/be ejected from the I^{-*} CTTS excited state, we fit the measured transients in Figure 4a with a simple kinetic model assuming only first-order growth of the electron population

$$I^-* \xrightarrow{k_1} I + e^-_{THF} \qquad (3)$$

Our fit included convolving the exponential appearance of the electrons with our measured $\sim$220 fs wide pump−probe pulse cross correlation. The result of this fit, shown as the black curves in Figure 4a, yielded an electron population appearance time of $1/k_1 = 380 \pm 60$ fs. This time for electron ejection from the CTTS excited state of I^- in THF is similar both to the electron ejection time scale following CTTS excitation of Na^- in tetrahydrofuran[22] and to the time scale measured for photoinduced relocalization of the e^-_{THF}.[15−17,19] Thus, the measurements in Figure 4a strongly support the idea that no matter how it is prepared, for example, via CTTS excitation of Na^- or I^- or via direct excitation of e^-_{THF}, the excited state(s) of an excess electron in liquid THF take $\sim$400 fs to undergo the transition required to relax the electron into the localized ground state of one of the preexisting cavities. Once the ground state is reached, the electron is already nearly completely equilibrated. Furthermore, because the electron may reside in a cavity far from where it originated, any memory of how the excited state was prepared is essentially lost. Thus, we believe that it is solely the structure of liquid THF, with its readily accessible disjoint excited states
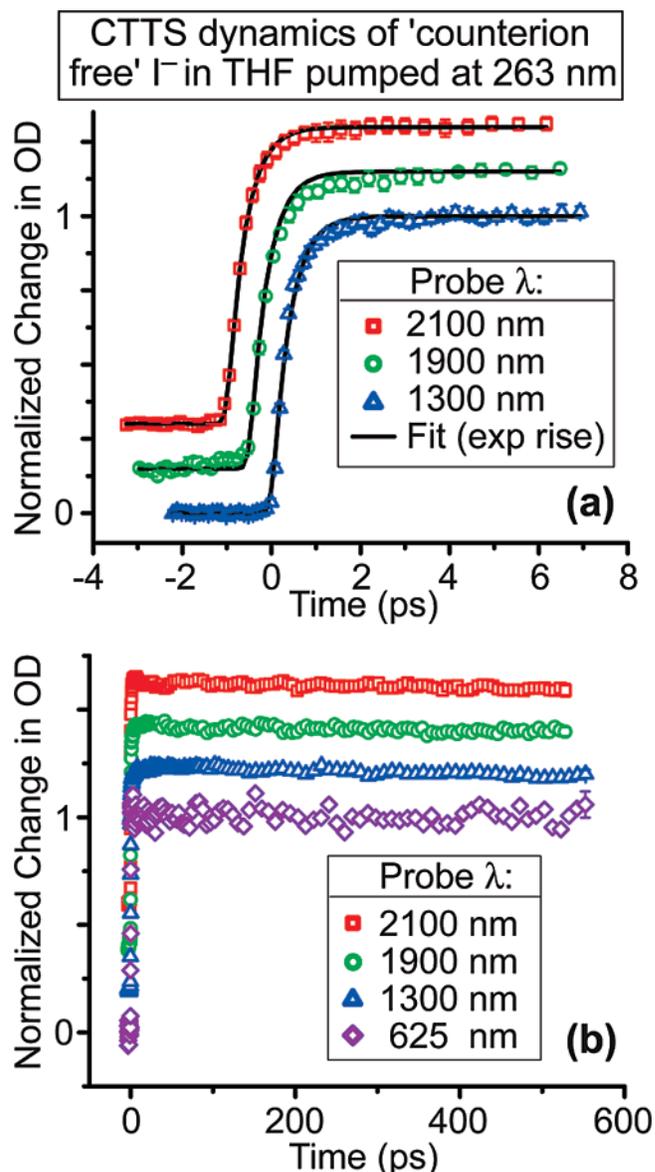
Figure 4. Ultrafast transient absorption dynamics of the solvated electron measured at selected infrared and visible wavelengths following 263 nm CTTS excitation of NaI/THF solutions containing excess 18-crown-6 ether. (a) Early time appearance dynamics of THF-solvated electrons created following CTTS excitation of I^- (colored symbols); the transients are fit by a common single-exponential rise with a time constant of 380 ± 60 fs, convolved with our $\sim$220 fs temporal resolution (solid black curves). The absorption transients are plotted offset in both dimensions for clarity; the 1300 nm transient is plotted properly with respect to the axis labels. (b) Long-time population dynamics of THF-solvated electrons created following CTTS excitation of I^- (colored symbols). In this panel, the magnitude of the transients has been normalized to the average intensity at $t > 300$ ps and offset vertically for ease of comparison. No observable change occurs for all transients on this $\leq$500 ps time scale, indicating a lack of diffusive geminate recombination for the "free" I^-/THF CTTS system. The early time dynamics at 650 nm is not shown in (a) due to a large coherence artifact that obscures the electron appearance dynamics.

and preexisting electron traps, that determines the relaxation dynamics of excited excess electrons; we always observe identical relaxation dynamics in THF independent of the details of the electronic structure of the solute furnishing the electron.

Figure 4b demonstrates that the spectral transients collected after pumping the lowest-energy CTTS transition of "free" I^- in THF at 263 nm are also identical on longer time scales and that there is negligible decay of the electrons over hundreds of

Ultrafast CTTS Dynamics of Iodide in THF

J. Phys. Chem. B, Vol. 112, No. 2, 2008 **489**

picoseconds.[83] This result indicates a nearly complete absence of geminate recombination of the ejected electrons with their neutral I atom partners. This behavior is surprisingly different from both the dynamics of hydrated electrons generated via the CTTS excitation of aqueous I^-, of which $\sim$70% undergo geminate recombination by 100 ps (cf. Figure 1b),[2,3] and the dynamics of electrons generated via the CTTS excitation of Na^- (and also K^-)[84] in THF, which recombine significantly with their neutral-atom partners on both $\sim$1 and $\sim$200 ps time scales (cf. Figure 1d). We note that recombination is particularly prominent when Na^- is excited along the red edge of its CTTS band,[10] similar to the excitation conditions for the I^- data presented in Figure 4. Perhaps even more surprising is the fact that we observe less recombination following the CTTS excitation of I^- in THF than we do from the multiphoton excitation of neat liquid THF with $\sim$5 eV of excess excitation energy (see ref 14 as well as section III.D below). This leads to the question of why is there so little recombination of the electrons ejected from I^- in THF, which we address in the following subsections.

C. Scavenging of the Ejected Electrons and the I^{-*} CTTS Excited State in THF. The fact that the transients presented in Figure 4 lack any signature of geminate recombination of CTTS-ejected electrons to re-form I^- poses the question of "where are the ejected electrons?" Do the CTTS-generated electrons reside near their iodine atom partners in contact pairs, bound together by a potential of mean force but separated by a barrier to recombination that is large compared to k_BT at room temperature? Or, are all of the electrons ejected so far from their I atom partners that they simply cannot diffuse back on subnanosecond time scales? To address these questions, we undertook a series of electron scavenging experiments devised to determine the distribution of distances at which the electrons reside immediately following their CTTS ejection from I^- in THF. The idea underlying these experiments is straightforward; assuming that the scavenger molecules are uniformly distributed throughout the fluid at a known concentration, we can monitor the number of electrons that encounter the scavengers as a function of time and thus determine the volume over which the electrons were initially distributed.[85,86]

The results of our scavenging experiments are summarized in Figure 5; in these experiments, we monitored the population of electrons via their absorption at 2050 nm as a function of time following the 263 nm CTTS excitation of I^- in THF in the presence of chloroform ($CHCl_3$). We chose $CHCl_3$ since it is an ideal scavenger of electrons in aprotic solvents[28] and is also miscible with THF. Figure 5a illustrates that there are two main effects observed as the amount of added $CHCl_3$ scavenger is increased. First, rather than remaining constant with time (cf. Figure 4b), the electron population decays on a tens-to-hundreds-of-picoseconds time scale due to diffusive encounters of the ejected electrons with the scavengers; as expected, the decay rate increases with increasing scavenger concentration. Second, the total number of ejected electrons we see (i.e., the maximum magnitude of the absorption signal) decreases with increasing scavenger concentration. This decrease is due to so-called "static quenching", whereby the CTTS excited state transfers an electron to the scavenger before detachment is complete, such that the total number of electrons that are ultimately ejected is reduced. We consider each of these two effects in turn.

The first of these processes, the diffusive encounter of the CTTS-ejected electrons with the scavengers, is highlighted in Figure 5b, which presents the same data as those in Figure 5a but with the transients normalized at $t = 10$ ps to better illustrate
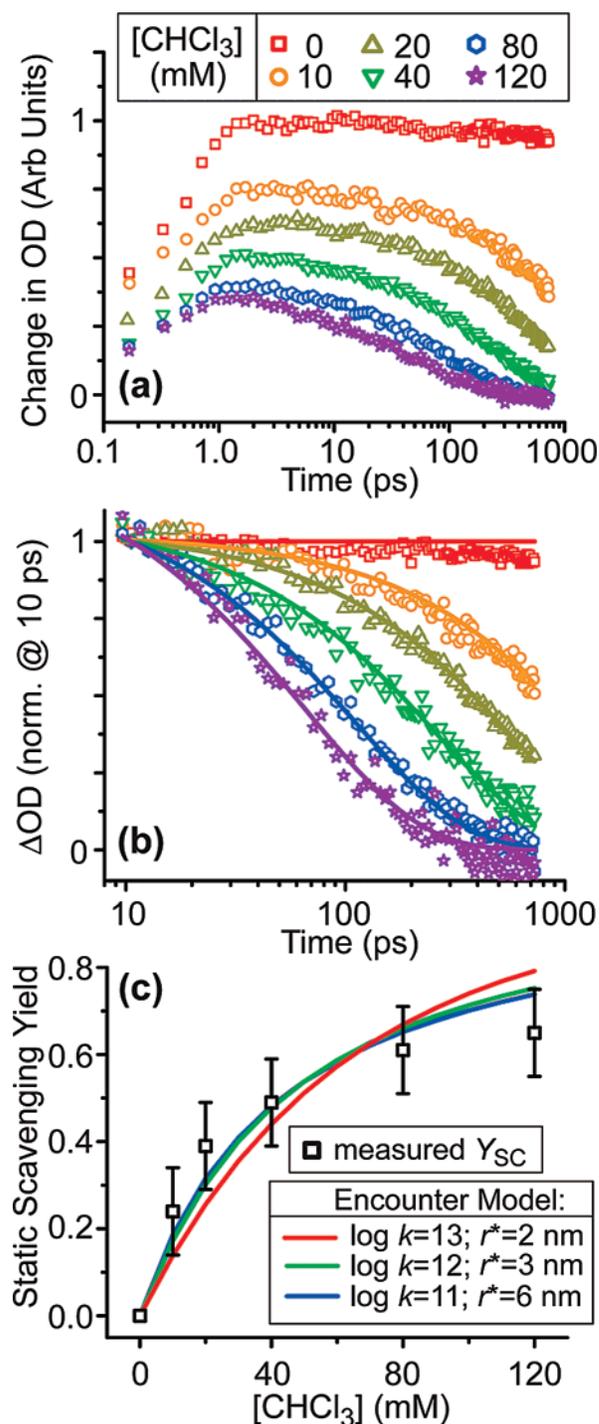
Figure 5. Scavenging kinetics of the THF-solvated electron and I^- CTTS excited state by $CHCl_3$ probed at 2050 nm following 263 nm CTTS excitation of "counterion-free" I^- in THF. (a) Electron absorption dynamics in the presence of various concentrations of $CHCl_3$ (colored symbols), normalized relative to the intensity of the signal with no $CHCl_3$ present (red squares). The presence of scavengers results both in loss of e^-_{THF} population due to diffusive encounters, as seen by the long-time absorption decay, and in "static scavenging" of the I^- CTTS excited state, as observed by the reduction in the maximum absorption intensity recorded at a given scavenger concentration. (b) Same data as those in (a), but with the absorption transients normalized at $t = 10$ ps. The solid curves are fits to solutions of the Smoluchowski equation for a homogeneous scavenger concentration and a fitted reaction distance of 8 ± 1 Å; see text for details. (c) Excited-state scavenging yields, Y_{sc} (squares with error bars; i.e., the fraction that the absorption signal is reduced at $t = 1$ ps), plotted against scavenger concentration. The colored curves are fits with a dynamic encounter model explained in the text.

the scavenging kinetics on longer time scales. If the distribution of scavengers in the liquid is homogeneous and there is no competing recombination with the I atom parent (as we believe is the case from Figure 4b), then the scavenging kinetics should be adequately modeled by the Smoluchowski equation for diffusion[87,88]

$$\Omega(t) = \Omega_0 \exp\{-4\pi RD[S] \, (1 + 2R/\sqrt{\pi Dt})t\} \qquad (4)$$

where Ω_0 and $[S]$ are the (relative) initial electron population and scavenger concentrations, respectively, and D is the relative diffusion constant between the electron and the chloroform scavenger. This model assumes that scavenging occurs instantaneously and with unit probability once the electron and scavenger encounter each other at a distance R. If we estimate the diffusion constant of $CHCl_3$ in THF as being roughly equal to the self-diffusion constant of THF, 3.5×10^{-5} cm^2/s,[89] and use the calculated value of the THF-solvated electron's diffusion constant, 7.6×10^{-5} cm^2/s,[90] then we can simultaneously fit all five scavenging traces using a single, physically reasonable value for the encounter radius of 8 ± 1 Å; the fits are shown as the solid curves through the data in Figure 5b.[91] The quality of the fit achieved with this simple recombination model suggests that the ejected electrons are indeed freely diffusing and that it is unlikely that any significant fraction of them are tightly bound in contact pairs with their iodine atom partners.

As we know from Figures 4 and 5b that nascent electrons do not recombine with their I atom partners and diffuse freely, where are they with respect to the iodine atom immediately after they relax from the I$^-$* CTTS excited state? We can answer this question by investigating the second scavenging process, the static quenching of the CTTS excited state. The (relative) reduction in the maximum amplitude of the electron absorption signal (at 1 ps) in Figure 5a with increasing scavenger concentration gives the excited-state scavenging yield; this quantity is plotted in Figure 5c. We can model these excited-state scavenging yields using an electron/scavenger encounter-complex model elaborated by Barbara and co-workers.[85] In this model, the scavenger yield, Y_{sc}, is given by

$$Y_{sc} = \sum_{n=1}^{\infty} \frac{n k_{ET} f_n}{(n k_{ET} + 1/\tau)} \qquad (5)$$

in which the nth term of this sum corresponds to a simultaneous encounter of the excited state with n scavengers, k_{ET} is the quenching rate per scavenger, and τ is the CTTS excited-state lifetime. In eq 5, f_n is the probability of the excited state interacting simultaneously with n scavengers. If the distribution of scavengers is homogeneous, then f_n can be modeled with a Poisson distribution

$$f_n = \frac{\bar{N}^n \exp^{-\bar{N}}}{n!} \qquad (6)$$

where $\bar{N}$ is the average number of scavengers within the volume of the encounter complex

$$\bar{N} = (1000[S])N_A \cdot (4/3)\pi r^{*3} \qquad (7)$$

in which r^* is the radius (in m) of the electron−scavenger encounter complex, $[S]$ is the scavenger concentration (in M), and N_A is Avogadro's number. Formally, r^* is a sum of effective scavenger and excited-state radii, but as we expect the size of the CTTS excited state to be large compared to the size of a

single chloroform scavenger, we can safely neglect the radius of the scavenger.

When fitting our data to this model, our goal is to extract the excited-state radius, r^*, but we also do not know the excited-state scavenging rate, k_{ET}.[92] Consequently, our fitting of the six data points in Figure 5c to obtain both of these parameters is poorly constrained. Thus, to obtain an order-of-magnitude estimate to the size of the I$^-$* CTTS excited state, we applied this model to our data by treating the excited-state radius as a fitting parameter while fixing the scavenging rate to a series of physically reasonable values (i.e., assuming scavenging times k_{ET}^{-1} between 100 fs and 10 ps). With this approach, we find that r^* must be large (at least several nanometers) and k_{ET} must be relatively small ($\leq 10^{12}$ sec^{-1}) in order to match both the magnitude and curvature of the concentration-dependent scavenging yields. The best fit (green) curve plotted in Figure 5c corresponds to $r^* = 6.3$ nm when we choose $k_{ET} = 10^{11}$ sec^{-1}. Even if we try to force a fit to the data with a very fast scavenging rate (10^{13} sec^{-1}, red curve), we still find that the excited-state radius must be at least 2 nm and that the corresponding fit passes outside of the conservative error bars. Consequently, this analysis suggests that the I$^-$* CTTS excited state in THF must be at least a few nanometers in radius to explain the static scavenging yields measured experimentally.[93]

This result, that the electrons are ejected to a large distance following CTTS excitation of I$^-$ in THF, is quite surprising, particularly since Bradforth and co-workers found that the CTTS excitation of aqueous iodide led to the formation of contact pairs with the solvated electrons adjacent to the iodine atom.[1−5] To us, this result suggests that the CTTS excited state of I$^-$ is strongly coupled to the naturally occurring disjoint states in liquid THF. If CTTS excitation leads to rapid population of one of the disjoint states, then the effective radius of the excited state is the distance of the preexisting cavities that the disjoint excited electron can sample, which simulations suggest is indeed a few nanometers.[59,61] Moreover, since the electron in a disjoint state is delocalized between multiple cavities, the electron density in any one cavity is small. This implies that the overlap between the excited electron and any scavengers adjacent to the cavities also will be small, consistent with the relatively slow excited-state scavenging rate implied by our modeling of the static quenching data. Thus, we conclude that the large amount of excited-state quenching observed results from a relatively slow per-scavenger quenching rate that is offset by the considerable number of scavengers available within the large volume accessible to the electron in its disjoint excited states.

D. Understanding the (Lack of) Recombination in the CTTS Dynamics of I$^-$ in THF. The scavenging data in Figure 5 imply both that the electrons ejected following the CTTS excitation of I$^-$ in THF diffuse freely and that the electrons are ejected to a distance of several nanometers from the iodine atom core. In this subsection, we explore the consistency of the scavenging results with the nearly complete lack of recombination observed in Figure 4b. Can the lack of recombination be explained quantitatively by the very large initial separation through which the geminate pair must diffuse to re-form I$^-$? Or, is it possible that there is a large barrier to recombination, even after the electron and iodine atom come into contact? To address these questions, we will compare the recombination dynamics of electrons generated via the CTTS excitation of I$^-$ in THF to those generated by multiphoton ionization of the neat solvent.

Figure 6 plots the population dynamics of electrons created via the 263 nm CTTS excitation of I$^-$ in THF (blue diamonds;

Ultrafast CTTS Dynamics of Iodide in THF

J. Phys. Chem. B, Vol. 112, No. 2, 2008 **491**
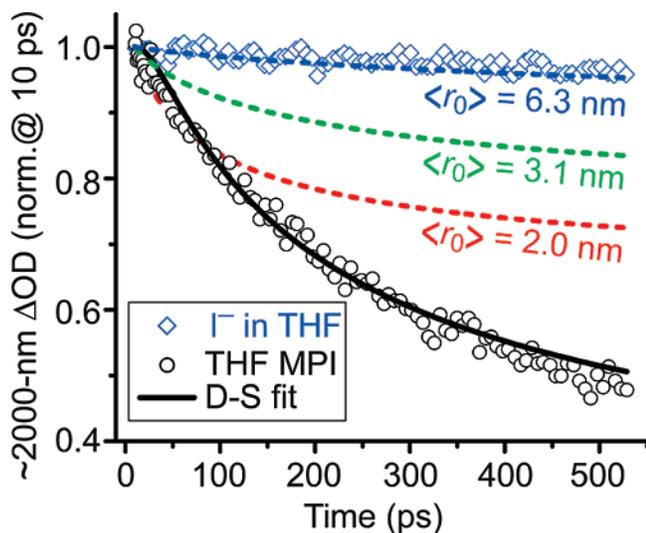
Figure 6. Long-time geminate recombination behavior of photo-generated solvated electrons in THF probed at ~2000 nm: recombination dynamics of e^-_{THF} with THF radical cations following 263 nm multiphoton ionization of neat THF at 263 nm (black circles); recombination dynamics of e^-_{THF} following 263 nm CTTS excitation of "counterion-free" I^- in THF (blue diamonds); the two data sets are normalized at $t = 10$ ps for ease of comparison. The solid black curve is a fit to an approximate solution to the Debye–Smoluchowski equation assuming an initial e^-_{THF}–cation average separation of 37 Å, a reaction distance of 11 Å, and a reaction velocity of 0.12 Å/ps. The three colored dashed curves illustrate the expected diffusion-limited recombination for e^-_{THF} with iodine, assuming an 8 Å reaction distance and an initial Gaussian distribution of e^-_{THF}–iodine atom separations with $\langle r_0 \rangle$ of 20, 31, and 63 Å (red, green, and blue, respectively).

same data as those in Figure 4b) and via the 263 nm multiphoton ionization (MPI) of pure THF (black circles); the two traces are normalized at $t = 10$ ps for ease of comparison. The MPI transient shows a significant decrease in the electron population on a hundreds-of-picoseconds time scale, the result of geminate recombination between the residual THF radical cation and the ejected solvated electron.[94] The observed decay of the electron population is similar in time scale and magnitude to that seen in earlier experiments in which the MPI of THF was accomplished with visible light pulses rather than UV pulses at 263 nm.[14] In this previous work, the electron population dynamics were well described by an approximate solution to the Debye–Smoluchowski equation,[95,96] and fits to the data yielded a reaction distance of 11 ± 1 Å, a reaction velocity of 1.2 ± 0.2 m/s, and an initial electron ejection length, r_0, of 40–45 Å.[14] If we utilize the values of the reaction distance and velocity from this previous work to analyze the 263 nm MPI of THF data in Figure 6, we obtain an excellent Debye–Smoluchowski fit with an initial electron ejection length of $r_0 = 37$ Å; this fit is shown as the solid black curve through the data. This ejection distance suggests that the 263 nm MPI of neat THF does not likely take place via a two-photon process, which would provide less than 1 eV of excess energy to the ejected electron. Rather, it is more likely that MPI of THF at 263 nm occurs through a three-photon process, providing ~5.5 eV of excess energy above the ~8.5 eV ionization potential of liquid THF, leading to similar dynamics and initial ejection distances to those observed previously with comparable excess energies by the four- and five-photon MPI of THF with visible wavelengths.[14]

The observation that the recombination dynamics following the CTTS excitation of I^- are so different than those following

the MPI of the solvent has several important implications for our study of the CTTS process. First, and foremost, the fact that we see faster recombination in the case of MPI (along with the linear power dependence of the CTTS absorption signals; see section II) verifies that we are not studying a mixture of CTTS and solvent MPI dynamics in our CTTS experiments. Importantly, our MPI recombination kinetics were measured under tighter focusing conditions than those used to study I^- CTTS, and the magnitude of the MPI transient absorption was much weaker than that following CTTS excitation. Second, the fact that there is less recombination of the CTTS electrons strongly suggests that the CTTS ejection distance is comparable to or greater than that produced by MPI. Of course, the electron is coulombically attracted to the THF radical cation in the case of MPI and there is no long-range attraction between the electron and its parent iodine atom in the case of CTTS. Consequently, we can use a simple Smoluchowski model to quantify the diffusive recombination expected in the case of CTTS. The three dashed curves in Figure 6 give the expected electron population dynamics assuming an initial Gaussian electron ejection distribution centered on the anion,[97] with the mean ejection distance, $\langle r_0 \rangle$, chosen to match the three distances we obtained when fitting the excited-state scavenging yields in Figure 5c with different scavenging rates. Here, we have assumed the same mutual diffusion coefficient (1.1×10^{-5} cm^2/s) and reaction distance (8 Å) used to fit the long-time scavenging data presented in section III.C. All of the traces are normalized at 10 ps for comparison. Figure 6 demonstrates that ~27, 17, and 5% of electrons should recombine if $\langle r_0 \rangle$ is chosen to be 20, 31, or 63 Å, respectively; as expected, less recombination should occur as the initial separation of geminate pairs is increased.

This modeling supports the idea that (if the recombination of the electrons generated via the CTTS excitation of I^- in THF is simply diffusion-controlled, then) the initial ejection distance of the electrons must be at least several nanometers, consistent with what we found from the excited-state scavenging yields in Figure 5c. However, what if the recombination is not diffusion-controlled? Could there be an attractive potential of mean force holding the electron near the iodine atom and/or a significant barrier to recombination? Bradforth and co-workers have described the recombination of aqueous electrons with iodine atoms as occurring on a potential of mean force, with the yield determined by a competition between recombination over a barrier and diffusive escape of the geminate partners that are bound in an attractive well.[3,5] However, if there were a potential of mean force that could partially hold the electron in the vicinity of the iodine atom in THF, we would not expect to be able to fit the dynamic scavenging experiments in Figure 5b with a model that assumes freely diffusing solvated electrons. It is also certainly possible that there is a barrier to recombination in THF and that this barrier could be larger in THF than that in H_2O since the amount of electron–iodine recombination has been observed to decrease as the polarity of the solvent decreases.[5] At this point, the question as to whether or not recombination can take place quickly or requires crossing a significant barrier once diffusion is complete remains open. However, the data and analysis in Figures 4–6 provide a compelling case that the CTTS excitation of I^- in THF leads to an average electron ejection distance of several nanometers, explaining the lack of observed geminate recombination. Thus, to the best of our knowledge, virtually no CTTS-ejected electrons encounter their iodine atom partners in THF on subnanosecond time scales.

IV. Discussion: Understanding the Roles of the Solute and Solvent in CTTS Dynamics

In the previous section, we examined the dynamics of electron ejection following the CTTS excitation of I^- in liquid THF. We found that it takes ∼400 fs for the electron to be ejected following CTTS excitation and that the ejected electrons appear with their equilibrium spectrum (Figure 4a). We also found that the ejected electrons reside, on average, several nanometers away from their iodine atom parents (Figure 5), such that no geminate recombination occurs on subnanosecond time scales (Figures 4b and 6). This behavior is significantly different from that of aqueous I^-, from which electron ejection occurs in ≤100 fs; there is significant solvation of the ejected electrons on a ∼1 ps time scale, and the majority of the ejected electrons recombine with their I atom partners in ∼100 ps (cf. Figure 1b).[1−5] The recombination dynamics following CTTS excitation of I^- in THF are also quite different from those of Na^- in THF,[10−22] although the electron ejection time and lack of solvation following ejection are similar for these two solutes (cf. Figure 1d). In this section, we present a picture designed to rationalize the similarities and differences in the CTTS dynamics of these three related systems.

Figure 7 presents an illustrative energy level diagram based on our understanding of the structures of liquid water and THF and the electronic structures of the Na^- and I^- CTTS solutes. In this figure, the colored lines represent bound states of the solute or CTTS states that are bound locally within the solvent cavity containing the solute. The gray-scaled bands represent a continuum of electron energy levels associated with the neat solvent (i.e., levels that exist independent of the solute, which are usually referred to as continuum levels or the solvent conduction band), with darker colors corresponding to a higher density of states. As discussed above and in ref 59, liquid THF is filled with preexisting cavities that act as electron traps, leading to the existence of low-lying disjoint states that may be thought of as a gradual onset to the liquid conduction band, as illustrated on the left side of Figure 7. Liquid water, on the other hand, lacks naturally existing cavities,[62] and the conduction band onset is more abrupt, as shown on the right side of Figure 7. We stress that the level diagrams in Figure 7 are meant to be qualitative in nature, as neither the absolute energies of these levels nor the relation between them in the two solvents is known from either experiment or theory. Nonetheless, we believe that the qualitative picture provided by Figure 7 can explain all of the salient features associated with the CTTS dynamics of the Na^-/THF, I^-/THF, and I^-/H_2O CTTS systems.

The electronic ground state of Na^- has the excess electron in a 3s orbital, suggesting that the solvent-bound CTTS excited states should be p-like. Indeed, pump−probe polarized hole-burning[98,99] measurements are largely consistent with the idea that Na^- has three p-like CTTS excited states whose energies are split by the local asymmetry of the solvent environment.[12,20,21] When sodide is excited on the red edge of its CTTS band (ca. 900 nm), 100% of the ejected electrons recombine with their Na^0 partners within ∼1 ps,[13] suggesting that all of these electrons were ejected within the same solvent cavity containing the Na^0 solute in what we refer to as immediate contact pairs. Thus, we believe that the lowest-energy CTTS state of Na^- must lie below the energy of the lowest accessible disjoint state in liquid THF, as depicted in Figure 7. When Na^- is excited at higher energies across its CTTS absorption band, an increased fraction of the CTTS-ejected electrons does not undergo rapid recombination (cf. Figure 1c).[13] This suggests that the higher-lying CTTS excited states can undergo rapid
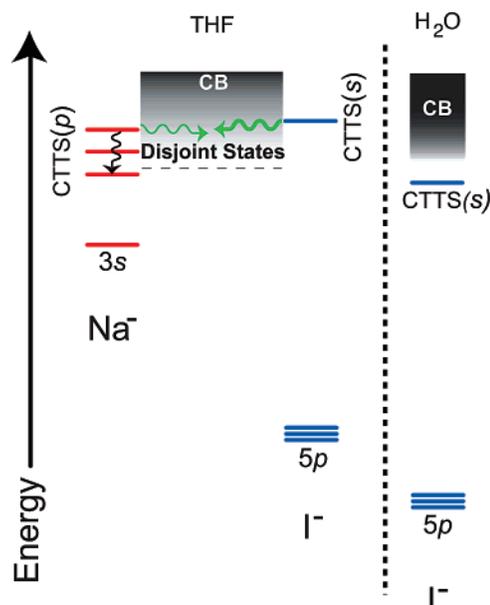
Figure 7. Schematic rationalizing the CTTS and solvent-supported level energetics of Na^- in THF and I^- in both THF and water. Colored solid lines represent anion-centered bound states (i.e., CTTS states). The graded bands (gray) represent solvent-supported excited states of the neat liquid, with the shading proportional to the density of states. Liquid THF is characterized by a gradual onset of solvent-supported states, ranging from disjoint states, bound by two or more preexisting electropositive cavities that naturally exist in liquid THF, to the conduction band continuum (CB). In contrast, the tightly packed structure of liquid water is characterized by a sharp onset of conduction band states. The s-like CTTS excited state of I^- in water is below the CB onset, such that CTTS-generated electrons can only be ejected nearby their iodine atom partners with significant structural rearrangement of the solvent. The s-like CTTS excited state of I^- in THF, on the other hand, lies well within the manifold of disjoint states (energetically), such that strong nonadiabatic coupling (wiggly green arrow) rapidly leads to relocalization of the CTTS-excited electron to other cavities in the fluid; little additional solvent reorganization is required to accommodate these nascent electrons. The lowest p-like CTTS excited state of Na^- in THF lies below the lowest disjoint state so that excitation to higher-lying CTTS excited states produces a competition between nonadiabatic relocalization into other cavities (wiggly green arrow) and internal conversion to the lowest state (wiggly black arrow), resulting in a strong pump excitation wavelength dependence to the electron ejection distance. This diagram is meant to be qualitative in nature; the dashed line separating the THF and H_2O schemes is drawn to imply that they are not to be compared on an absolute scale.

nonadiabatic coupling to disjoint states with comparable or lower energies,[61] allowing the excited electrons to relax into cavities farther from the sodium core. We believe that the relaxation mechanism is similar to the relocalization of excited THF-solvated electrons that has been observed in both experiments[15,16,19] and simulations.[61] However, simulations also suggest that excitation of higher-lying CTTS excited states can lead to rapid internal conversion to the lowest-energy CTTS state.[23−25,100] Thus, we believe that when the electron is promoted to one of the higher-lying CTTS states, there is a kinetic competition between coupling into one of the disjoint states (as depicted by the wiggly green arrow on the left side of Figure 7) and relaxation to the lowest CTTS state (depicted by the black wiggly arrow on the left side of Figure 7). Since the density of the disjoint states increases at higher energies, the rate to nonadiabatically couple to a disjoint state should also increase, thus explaining the lowering of the CTTS recombination yield with increasing excitation energy. Furthermore, as argued above, the lack of solvation of the ejected electrons can

Ultrafast CTTS Dynamics of Iodide in THF

J. Phys. Chem. B, Vol. 112, No. 2, 2008 **493**

be explained by the fact that the cavities into which the electron is ejected are preexisting, so that little additional relaxation is needed once the electron makes the nonadiabatic transition to its new ground state.[61]

In contrast, simulations suggest that (ignoring spin−orbit excitation of the neutral iodine atom product) aqueous I⁻ has only a single s-like CTTS excited state that can be accessed from its 5p electronic ground state.[58] Careful experiments by Bradforth and co-workers have determined that the energies of the conduction band states in liquid water lie above that of the I⁻ CTTS excited state[101] (as depicted in Figure 7), such that CTTS excitation of I⁻ in water can only produce electrons that remain localized near their iodine atom parents. This explains why the CTTS excitation of aqueous I⁻ produces contact pairs that can readily undergo recombination, which is controlled by their relative diffusion on the local potential of mean force.[3] Since liquid water contains no preexisting cavities, the ejected electron must force significant local solvent reorganization, explaining the marked spectral shifts observed following both CTTS excitation of aqueous iodide[4,9] and the multiphoton ionization of neat water.[4,65,68]

We propose that the CTTS dynamics of I⁻ in THF are sensibly explained if the single s-like CTTS excited state lies relatively high in the manifold of disjoint states energetically, as suggested at the center of Figure 7. Thus, CTTS excitation of I⁻ in THF leads to rapid nonadiabatic coupling to disjoint states (as depicted by the wiggly green arrow in Figure 7), such that few electrons relax to their ground states near their iodine atom partners. The marked contrast in recombination behavior from Na⁻ arises because I⁻ has no lower-lying CTTS excited states, so that there is no competition preventing all of the CTTS-excited electrons from relocalizing into new cavities via disjoint states. Even though this coupling must be strong, we can rationalize the fact that the CTTS spectrum of I⁻ in THF is so similar to that in water (cf. Figures 1a and 3) and other solvents because we know from simulations that there is little electronic overlap and thus little oscillator strength between a localized electronic ground state and the naturally occurring disjoint states in liquid THF.[59] Thus, we expect the disjoint states to be spectroscopically "dark" from the I⁻ ground state, such that the "bright" CTTS excited state carries all of the Franck−Condon oscillator strength. The similarity of the I⁻/THF CTTS spectrum to that in other solvents also suggests that the I⁻ CTTS excited state lies below the conduction band since strong coupling to the conduction band states would likely lead to a significant distortion of the CTTS absorption spectrum, unless most of the coupling takes place away from the Franck−Condon region. Finally, as was observed for Na⁻, there is no significant solvation of the CTTS-ejected electrons from I⁻ in THF because all of the ejected electrons relax into preexisting cavities.

In summary, we have demonstrated that chelation of the Na⁺ counterion with 18-crown-6 ether results in a considerable red shift of the I⁻ CTTS peak maximum, indicating that I⁻ can be prepared in a "counterion-free" environment in liquid THF. We found that the CTTS dynamics of "counterion-free" I⁻ in THF is characterized by the complete absence of both electron solvation and iodine−electron geminate recombination. The large (several nanometer) effective spatial extent of the excited state determined from the scavenging measurements indicates that CTTS electron ejection involves strong coupling between the localized CTTS excited state and the manifold of preexisting THF-supported disjoint electronic states. Consequently, the absence of iodine−electron recombination on subnanosecond time scales is largely due to the fact that there is insufficient time for diffusion to allow for a re-encounter between the geminate partners. The fact that the CTTS detachment and recombination dynamics of I⁻ in THF differ considerably from those associated with I⁻ in H₂O or Na⁻ in THF is thus a direct result of electronic structure differences of both the CTTS solute and the solvent.

References and Notes

(1) Kloepfer, J. A.; Vilchiz, V. H.; Lenchenkov, V. A.; Bradforth, S. E. *Chem. Phys. Lett.* **1998**, *298*, 120.

(2) Kloepfer, J. A.; Vilchiz, V. H.; Lenchenkov, V. A.; Germaine, A. C.; Bradforth, S. E. *J. Chem. Phys.* **2000**, *113*, 6288.

(3) Kloepfer, J. A.; Vilchiz, V. H.; Lenchenkov, V. A.; Chen, X.; Bradforth, S. E. *J. Chem. Phys.* **2002**, *117*, 766.

(4) Vilchiz, V. H.; Kloepfer, J. A.; Germaine, A. C.; Lenchenkov, V. A.; Bradforth, S. E. *J. Phys. Chem. A* **2001**, *105*, 1711.

(5) Vilchiz, V. H.; Chen, X.; Kloepfer, J. A.; Bradforth, S. E. *Radiat. Phys. Chem.* **2005**, *72*, 159.

(6) Lenchenkov, V.; Kloepfer, J.; Vilchiz, V.; Bradforth, S. E. *Chem. Phys. Lett.* **2001**, *342*, 277.

(7) Sauer, M. C.; Shkrob, I. A.; Lian, R.; Crowell, R. A.; Bartels, D. M.; Chen, X.; Suffern, D.; Bradforth, S. E. *J. Phys. Chem. A* **2004**, *108*, 10414.

(8) Moskun, A. C.; Bradforth, S. E.; Thøgersen, J.; Keiding, S. *J. Phys. Chem. A* **2006**, *110*, 10947.

(9) Iglev, H.; Trifonov, A.; Thaller, A.; Buchvarov, I.; Fiebig, T.; Laubereau, A. *Chem. Phys. Lett.* **2005**, *403*, 198.

(10) Barthel, E. R.; Martini, I. B.; Schwartz, B. J. *J. Chem. Phys.* **2000**, *112*, 9433.

(11) Barthel, E. R.; Martini, I. B.; Schwartz, B. J. *J. Phys. Chem. B* **2001**, *105*, 12230.

(12) Barthel, E. R.; Martini, I. B.; Keszei, E.; Schwartz, B. J. *J. Chem. Phys.* **2003**, *118*, 5916.

(13) Barthel, E. R.; Schwartz, B. J. *Chem. Phys. Lett.* **2003**, *375*, 435.

(14) Martini, I. B.; Barthel, E. R.; Schwartz, B. J. *J. Chem. Phys.* **2000**, *113*, 11245.

(15) Martini, I. B.; Barthel, E. R.; Schwartz, B. J. *Science* **2001**, *293*, 462.

(16) Martini, I. B.; Barthel, E. R.; Schwartz, B. J. *J. Am. Chem. Soc.* **2002**, *124*, 7622.

(17) Martini, I. B.; Schwartz, B. J. *Chem. Phys. Lett.* **2002**, *360*, 22.

(18) Martini, I. B.; Barthel, E. R.; Schwartz, B. J. *Pure Appl. Chem.* **2004**, *76*, 1809.

(19) Martini, I. B.; Schwartz, B. J. *J. Chem. Phys.* **2004**, *121*, 374.

(20) Wang, Z.; Shoshana, O.; Hou, B.; Ruhman, S. *J. Phys. Chem. A* **2003**, *107*, 3009.

(21) Shoshana, O.; Pérez Lustres, J. L.; Ernsting, N. P.; Ruhman, S. *Phys. Chem. Chem. Phys.* **2006**, *8*, 2599.

(22) Cavanagh, M. C.; Larsen, R. E.; Schwartz, B. J. *J. Phys. Chem. A* **2007**, *111*, 5144.

(23) Smallwood, C. J.; Bosma, W. B.; Larsen, R. E.; Schwartz, B. J. *J. Chem. Phys.* **2003**, *119*, 11263.

(24) Sheu, W.-S.; Rossky, P. J. *J. Phys. Chem.* **1996**, *100*, 1295.

(25) Sheu, W.-S.; Rossky, P. J. *Chem. Phys. Lett.* **1993**, *202*, 186.

(26) Staib, A.; Borgis, D. *J. Chem. Phys.* **1996**, *104*, 9027.

(27) Peon, J.; Hess, G. C.; Pecourt, J.-M. L.; Yuzawa, T.; Kohler, B. *J. Phys. Chem. A* **1999**, *103*, 2460.

(28) Xia, C.; Peon, J.; Kohler, B. *J. Chem. Phys.* **2002**, *117*, 8855.

(29) Serxner, D.; Dessent, C. E. H.; Johnson, M. A. *J. Chem. Phys.* **1996**, *105*, 7231.

(30) Becker, I.; Markovich, G.; Cheshnovsky, O. *Phys. Rev. Lett.* **1997**, *79*, 3391.

(31) Lehr, L.; Zanni, M. T.; Frischkorn, C.; Weinkauf, R.; Neumark, D. M. *Science* **1999**, *284*, 635.

(32) Verlet, J. R. R.; Kammrath, A.; Griffin, G. B.; Neumark, D. M. *J. Chem. Phys.* **2005**, *123*, 231102.

(33) Szpunar, D. E.; Kautzman, K. E.; Faulhaber, A. E.; Neumark, D. M. *J. Chem. Phys.* **2006**, *124*, 054318.

(34) Chen, H.-Y.; Sheu, W.-S. *Chem. Phys. Lett.* **2001**, *335*, 475.

(35) Takayanagi, T.; Takahashi, K. *Chem. Phys. Lett.* **2006**, *431*, 28.

(36) Timerghazin, Q. K.; Peslherbe, G. H. *Chem. Phys. Lett.* **2002**, *354*, 31.

(37) Blandamer, M. J.; Foster, M. J.; Hidden, N. J.; Symons, M. C. R. *Chem. Commun.* **1966**, 62.

(38) Blandamer, M. J.; Gough, T. E.; Symons, M. C. R. *Trans. Faraday Soc.* **1966**, *62*, 296.

(39) Blandamer, M. J.; Gough, T. E.; Symons, M. C. R. *Trans. Faraday Soc.* **1963**, *59*, 1748.

(40) Blandamer, M. J.; Gough, T. E.; Symons, M. C. R. *Trans. Faraday Soc.* **1966**, *62*, 286.

(41) Blandamer, M. J.; Fox, M. F. *Chem. Rev.* **1970**, *70*, 59.

(42) Fox, M. F.; Hayon, E. *Chem. Phys. Lett.* **1972**, *14*, 442.

(43) Griffiths, T. R.; Symons, M. C. R. *Trans. Faraday Soc.* **1960**, *56*, 1125.

(44) Griffiths, T. R.; Symons, M. C. R. *Mol. Phys.* **1960**, *3*, 90.

(45) Symons, M. C. R.; Jackson, S. E. *J. Chem. Soc., Faraday Trans. 1* **1979**, *75*, 1919.

(46) Sciaini, G.; Marceca, E.; Fernandez-Prini, R. *J. Phys. Chem. B* **2005**, *109*, 18949.

(47) Czapski, G.; Ottolenghi, M. *Isr. J. Chem.* **1968**, *6*, 75.

(48) Czapski, G.; Ogdan, J.; Ottolenghi, M. *Chem. Phys. Lett.* **1969**, *3*, 383.

(49) Farkas, A.; Farkas, L. *Trans. Faraday Soc.* **1938**, *34*, 1120.

(50) Dainton, F. S.; Logan, S. R. *Proc. R. Soc. London, Ser. A* **1965**, *287*, 281.

(51) Jortner, J.; Levine, R.; Ottolenghi, M.; Stein, G. *J. Phys. Chem.* **1961**, *65*, 1232.

(52) Jortner, J.; Ottolenghi, M.; Stein, G. *J. Phys. Chem.* **1962**, *66*, 2029.

(53) The transients plotted in Figure 1b were reconstructed using the fitting parameters presented in ref 2.

(54) Hart, E. J.; Boag, J. W. *J. Am. Chem. Soc.* **1962**, *84*, 4090.

(55) Jou, F.-Y.; Freeman, G. R. *Can. J. Chem.* **1979**, *57*, 591.

(56) Lok, M. T.; Tehan, F. J.; Dye, J. L. *J. Phys. Chem.* **1972**, *76*, 2975.

(57) Jou, F.-Y.; Dorfman, L. M. *J. Chem. Phys.* **1973**, *58*, 4715.

(58) Bradforth, S. E.; Jungwirth, P. *J. Phys. Chem. A* **2002**, *106*, 1286.

(59) Bedard-Hearn, M. J.; Larsen, R. E.; Schwartz, B. J. *J. Chem. Phys.* **2005**, *122*, 134506.

(60) Bowron, D. T.; Finney, J. L.; Soper, A. K. *J. Am. Chem. Soc.* **2006**, *128*, 5119.

(61) Bedard-Hearn, M. J.; Larsen, R. E.; Schwartz, B. J. *J. Chem. Phys.* **2006**, *125*, 194509.

(62) Rossky, P. J.; Schnitker, J. *J. Phys. Chem.* **1988**, *92*, 4277.

(63) Son, D. H.; Kambhampati, P.; Kee, T. W.; Barbara, P. F. *J. Phys. Chem. A* **2001**, *105*, 8269.

(64) Son, D. H.; Kambhampati, P.; Kee, T. W.; Barbara, P. F. *Chem. Phys. Lett.* **2001**, *342*, 571.

(65) Migus, A.; Gauduel, Y.; Martin, J. L.; Antonetti, A. *Phys. Rev. Lett.* **1987**, *58*, 1559.

(66) Kambhampati, P.; Son, D. H.; Kee, T. W.; Barbara, P. F. *J. Phys. Chem. A* **2002**, *106*, 2374.

(67) Yokoyama, K.; Silva, C.; Son, D. H.; Walhout, P. K.; Barbara, P. F. *J. Phys. Chem. A* **1998**, *102*, 6957.

(68) Hertwig, A.; Hippler, H.; Unterreiner, A. N.; Vöringer, P. *Ber. Bunsen-Ges. Phys. Chem.* **1998**, *102*, 805.

(69) Pshenichnikov, M. S.; Baltuška, A.; Wiersma, D. A. *Chem. Phys. Lett.* **2004**, *389*, 171.

(70) Bragg, A. E.; Schwartz, B. J. **2007**, in preparation.

(71) Mizuno, M.; Tanaka, J.; Harada, I. *J. Phys. Chem.* **1981**, *85*, 1789.

(72) Banin, U.; Ruhman, S. *J. Chem. Phys.* **1993**, *98*, 4391.

(73) Kühne, T.; Küster, R.; Vöhringer, P. *Chem. Phys.* **1998**, *233*, 161.

(74) Nguyen, T.-Q.; Martini, I. B.; Liu, J.; Schwartz, B. J. *J. Phys. Chem. B* **2000**, *104*, 237.

(75) Fox, M. F.; Hayon, E. *Chem. Phys. Lett.* **1974**, *25*, 511.

(76) Fox and Hayon did include THF in their 30-solvent study, placing the I⁻ CTTS band maximum at 40675 cm⁻¹, which is blue-shifted relative to our measurement under "counterion-free" conditions. Fox and Hayon did not state which I⁻ salt they used in their study, but we assume they used a salt containing a tetraalkylammonium countercation, which, as we will show in ref 70, still has some association with I⁻ in THF.

(77) Bhattacharyya, D. N.; Smid, J.; Szwarc, M. *J. Am. Chem. Soc.* **1964**, *86*, 5024.

(78) Chang, P.; Slates, R. V.; Szwarc, M. *J. Phys. Chem.* **1966**, *70*, 3180.

(79) Sinha, A.; Roy, M. N. *Phys. Chem. Liq.* **2007**, *45*, 67.

(80) Naturally, as the (18C6/Na⁺)−I⁻ CTTS spectrum was obtained from the measured composite by subtracting a scaled, measured Na⁺−I⁻ spectrum, the two add to recover the measured composite.

(81) If we relaxed our intensity−ratio condition for subtraction, the peak position of the extracted (18C6/Na⁺)−I⁻ spectrum varied by only ~1 nm, indicating that this stipulation is robust and minimally influences the value obtained.

(82) Figure 1c suggests that all of the transients shown in Figure 4 should reflect only the dynamics of the detached electrons, though we cannot rule out the possibility that at visible probe wavelengths, where the electron's

absorption cross section is small, there may be minor contributions from a weak charge-transfer-from-solvent (CTFS) band associated with nascent neutral iodine.[8,102] We note, however, that the population kinetics of the two must be identical according to the stoichiometry for geminate recombination: $I + e_{THF}^{-} \rightarrow I^{-}$. Because we would expect there to be a significant amount of dynamic solvation of the newly formed I atom (as there is for the neutral sodium atom left behind following the CTTS excitation of Na⁻),[21,22] the fact that we observe identical kinetics at 650 nm and in the IR suggests that absorption due to the CTFS band of I is negligible at this probe wavelength.

(83) The wavelength independence of these measured transients throughout the visible and infrared also indicates the absence of any type of transformation of the solvated electrons between cavity- and valence-bound motifs,[103,104] as has been observed in solution following CTTS excitation of I⁻ in acetonitrile.[28]

(84) Cavanagh, M. C.; Young, R.; Schwartz, B. J. **2007**, in preparation.

(85) Kee, T. W.; Son, D. H.; Kambhampati, P.; Barbara, P. F. *J. Phys. Chem. A.* **2001**, *105*, 8434.

(86) Pimblott, S.; LaVerne, J. A. *J. Phys. Chem. A.* **1998**, *102*, 2967.

(87) Smoluchowski, M. *Z. Phys. Chem.* **1917**, *92*, 129.

(88) Rice, S. A. Diffusion-Limited Reactions. *Chemical Kinetics*; Elsevier: Amsterdam, The Netherlands, 1985; Vol. 25.

(89) Helfrich, J.; Hentschke, R. *Macromolecules* **1995**, *28*, 3831.

(90) The mobility of e_{THF}^{-}, μ, has been measured as 3×10^{-3} cm²/Vs.[105] The e_{THF}^{-} diffusion constant, D, has been calculated[14] using Einstein's relation, $D = (k_{B}T/e)\mu$, in which e is the elementary charge, T is room temperature, and k_{B} is Boltzmann's constant.

(91) Even if we assume that the relative diffusion is dominated entirely by the electron, the data in Figure 5b are still well-fit with a 10 Å reaction radius, which corresponds to ~2 solvent shells in THF.

(92) We note that Barbara and co-workers were able to use this model to extract the size-dependent scavenging rates of various excited states of the $e_{H_{2}O}^{-}$[85] because the electronic radii were known from independent measurements.[86]

(93) Binary solution environments do introduce the possibility of preferential ion solvation.[38] For the solutions used in these scavenging experiments, preferential solvation of I⁻ by chloroform could result in a substantial scavenging enhancement. We note that we could not measure an observable shift in the I⁻ CTTS spectrum with the addition of chloroform at the highest concentration used in scavenging experiments (~1 % mole fraction), which suggests that the chloroform negligibly influences the immediate environment of the CTTS anion. Furthermore, we anticipate that dynamic scavenging highlighted in Figure 5b would not exhibit kinetics consistent with a diffusion model using the (homogenous) bulk scavenger concentration if a significant concentration enhancement near I⁻ existed. Also, we expect that the measured static scavenging yield would have a steep onset at low concentrations if there were strong I⁻−chloroform interactions. Finally, assuming a twofold increase in the average chloroform concentration within the CTTS-excited state volume, r^* would only change by a factor of $\sqrt[3]{1/2} \approx 0.8$ to give the same Y_{sc}. Therefore, we anticipate that any local concentration enhancement should not appreciably affect the nanometer size of the excited-state distribution obtained from this analysis.

(94) There is some evidence that suggests that the THF radical cation undergoes rapid chemistry with neighboring THF molecules subsequent to MPI,[14] such that the electron may recombine with a molecule that was not the original parent, as is the case for the multiphoton ionization of water.[106,107]

(95) Green, N. J. B. *Chem. Phys. Lett.* **1984**, *107*, 485.

(96) Green, N. J. B.; Pilling, M. J.; Clifford, P. *Mol. Phys.* **1989**, *67*, 1086.

(97) Clifford, P.; Green, N. J. B.; Pilling, M. J. *J. Phys. Chem.* **1982**, *86*, 1318.

(98) Cavanagh, M. C.; Martini, I. B.; Schwartz, B. J. *Chem. Phys. Lett.* **2004**, *396*, 359.

(99) Schwartz, B. J.; Rossky, P. J. *Phys. Rev. Lett.* **1994**, *72*, 3282.

(100) Sheu, W.-S.; Rossky, P. J. *J. Am. Chem. Soc.* **1993**, *115*, 7729.

(101) Bradforth, S. E. Private communication.

(102) Fornier de Violet, P.; Bonneau, R.; Joussot-Dubien, J. *Chem. Phys. Lett.* **1973**, *19*, 251.

(103) Mitsui, M.; Ando, N.; Kokubo, S.; Nakajima, A.; Kaya, K. *Phys. Rev. Lett.* **2003**, *91*, 153002.

(104) Shkrob, I. A.; Takeda, K.; Williams, F. *J. Phys. Chem. A* **2002**, *106*, 9132.

(105) Dodelet, J.-P.; Freeman, G. R. *Can. J. Chem.* **1975**, *53*, 1263.

(106) Goulet, T.; Jay-Gerin, J.-P. *J. Chem. Phys.* **1992**, *96*, 5076.

(107) Clifford, P.; Green, N. J. B.; Pilling, M. J. *J. Phys. Chem.* **1984**, *88*, 4171.